Biochemistry and Biophysics Reports 40 (2024) 101861

Contents lists available at ScienceDirect

Biochemistry and Biophysics Reports

journal homepage: www.elsevier.com/locate/bbrep

Structural modeling of phosphatidylinositol 3-kinase-γ with novel derivatives of stilbenoids

Sagar Rathee, Madhan Vishal Rajan, Simran Sharma, Gururao Hariprasad *

Department of Biophysics, All India Institute of Medical Sciences, Ansari Nagar, New Delhi, 110029, India

ARTICLE INFO

Keywords:
Phosphatidylinositol 3-kinase γ
Stilbenoids
Drug target
Structural based drug design
Interactions
Potency
Specificity

ABSTRACT

Phosphatidylinositol 3-kinases (PI3K) form a family of lipid kinases that catalyze the phosphorylation of 3-hydroxyl group of the inositol ring of phosphatidylinositol and its derivatives. It is implicated in inflammatory disorders and cancer thus making it an attractive drug target. Crystal structure of human PI3Kγ was taken and structure was completed using MODELLER and validated using PROCHECK. Stilbenoid molecules, piceatannol and resveratrol, were docked to kinase domain of PI3Kγ using AutoDock Vina and docked complexes were subjected to molecular dynamic simulations using Desmond suite of programmes. Based on the structural analysis of these complexes, modified derivatives of the native molecules were designed, docked and molecular dynamic simulations were performed. Kinase domain has a bi-lobar structure with ATP binding site lying in the cleft connecting the two lobes that are primarily composed of 12 α-helices and 8 β-strands. Piceatannol and resveratrol bind at the ATP binding site, with one its rings in a position primarily occupied by adenine of ATP making a hydrogen bond with backbone of Val882. Molecules also make interactions with Lys833 and several isoleucine residues. Interactions with Ser806 appear to be crucial for the loop conformation and compactness. Derivative molecules of stilbenoids also occupy the ATP binding cleft and the chemical modifications result in hydrogen bonded interactions to Glu880, and ionic interactions to Lys833 and Lys808 thereby enhancing their potencies in comparison to native molecules. Biophysical parameters and quality of interactions of stilbenoid derivatives augurs well for development of potent and specific inhibitory molecules against PI3Kγ enzyme.

1. Introduction

Phosphatidylinositol 3-kinases (PI3K) form a family of lipid kinases that catalyze the phosphorylation of 3-hydroxyl group of the inositol ring of phosphatidylinositol and its derivatives, namely phosphatidylinositol-4-phosphate and phosphatidylinositol-4,5-bisphosphate [1]. They are implicated in inflammatory disorders and cancer thus making it an attractive target for drug development [2–4].

PI3K enzymes have been classified into three classes based on substrate specificity, structure and mode of regulation [1,5]. Class I PI3Ks are an integral part of downstream signaling of various receptor tyrosine kinases (RTKs) and G-protein coupled receptors (GPCRs) [6]. They are heterodimeric proteins composed of a regulatory subunit and a catalytic subunit. They are further classified into subtypes A and B [7]. Class IA PI3Ks consist of a regulatory subunit p85, and a catalytic subunit p110 having three isoforms: p110α, p110β and p110δ, while Class IB PI3K consists of either p84 or a p101 as a regulatory subunit, and a single catalytic p110γ and called PI3Kγ [8]. Structural basis of binding of ATP and inhibitors like wortmannin, quercetin and myricetin to this enzyme have been elucidated [9].

Five PI3K inhibitors, namely Copanlisib, Idelalisib, Umbralisib, Duvelisib and Alpelisib have been approved by FDA and many other inhibitors are currently in various phases of clinical trials [10]. But none of the approved drugs are specific for PI3Kγ. Lack of specificity poses the threat of adverse side effects which has been observed in patients [11]. There is therefore a need to develop potent and specific inhibitors against PI3Kγ, a drug target in cancer and inflammation [2,4].

Natural molecules and their derivatives have been a leading source for pharmacologically active molecules and play an indispensable role in drug discovery [12]. This is mainly owing to the following advantages: (1) they are more diverse, novel, sterically more complex rendering more specificity to target binding; (2) they contain fewer nitrogen, halogen, and sulfur atoms but more oxygen atoms; (3) they have higher number of solvated hydrogen-bond donors and acceptors increasing binding affinity; (4) they have been optimized to have specific biological activity; (5) they are relatively safe and are less prone to

* Corresponding author.
E-mail address: dr.hariprasadg@gmail.com (G. Hariprasad).

https://doi.org/10.1016/j.bbrep.2024.101861
Received 27 September 2024; Received in revised form 22 October 2024; Accepted 27 October 2024

immunologically mediated allergies and adverse reactions; (6) more economically feasible for drug discovery and development [13].

Stilbenoids are a group of naturally occurring hydroxylated derivatives of stilbenes found in various berries and grapes. Resveratrol, a 3,5,4′-Trihydroxystilbene, has been found to be a molecule responsible for health benefits such as prevention of cardiovascular disease [14]. Piceatannol, 3,5,3′,4′-Tetrahydroxystilbene, is a natural analogue of resveratrol having beneficial effects in diseases, including cancer and neurodegenerative diseases [15,16]. Both, piceatannol and resveratrol, inhibits PI3K activity in both in vitro and ex-vivo assays, with piceatannol being more potent than LY294002, a well-known PI3Kγ inhibitor [17]. Interestingly, they also demonstrated that piceatannol and resveratrol competitively prevented ATP binding to inhibit the activity of PI3Kγ.

Our lab has been involved in the structural characterization of drug targets in the recent past. The outcomes have helped: to understand the structure-function relationship of drug target enzymes; to delineate the structural parameters required for potent drug design; development of natural molecules as drug candidates; structural implications of mutations, and provide structural basis for adverse effects of drug molecules [18–22]. In this study we look to provide a structural basis for the inhibition of PI3Kγ by stilbenoids and also provide stilbenoid scaffold-based derivatives as potent and specific inhibitors of PI3Kγ enzyme. The detailed structural analysis lays a platform for development of natural molecule drug candidates for cancer and inflammation.

2. Methodology

2.1. Sequence analysis

Protein sequences of human PI3K γ, α, β, and δ were taken from UniProtKB. Multiple sequence alignment of kinase domain was performed using Clustal Omega available at EMBL-EBI [23].

2.2. Modeling and validation

Crystal structure of γ-isoform of catalytic subunit PI3K was taken from Protein Data Bank (**PDB ID: 1E8Y**). Missing and incomplete residues were modelled using MODELLER [24]. Stereochemical correctness of selected model was analyzed using Ramachandran Plot, ERRAT and Verify 3D [25–28]. Kinase domain was then extracted from this structure, energy minimized using steepest descent method, and again validated using Ramachandran Plot, ERRAT and Verify 3D.

2.3. Receptor-ligand preparation and docking of piceatannol and resveratrol to PI3Kγ

Kinase domain of PI3Kγ was used as the receptor for docking studies. Receptor was prepared using PDB2PQR tool where charges were added using CHARMM27 force field and the protonation sites were determined using PropKa [29–31]. All ligands used in this study were prepared using AutoDockTools [32]. Piceatannol and resveratrol were used as ligands for the initial docking studies. Docking site was determined based on the binding pocket of ATP, wortmannin, myricetin and quercetin [9]. Targeted flexible docking was performed using AutoDock Vina where both, the ligand as well as side chains of binding site residues were kept flexible [32]. The docking grid with a dimension of 26 Å × 26 Å X 24 Å was used in docking calculation with an exhaustiveness option of 16. Scoring was performed using Vina Scoring Function which provides output results as Gibbs free energy of binding (ΔG). Binding affinity (K_d) was estimated using the equation: $\Delta G = -nRT.\ln K_d$, where ΔG stands for change in free energy of binding, R stands for Gas constant in calorie/mol/Kelvin, T stands for temperature in Kelvin, ln stands for natural log, and n stands for number of moles (calculated for 1 mol).

2.4. Molecular dynamics

MD simulation was performed by Desmond suite of programmes using force field parameters of OPLS3 [33,34]. Poses with lowest docking scores for piceatannol and resveratrol, and each of their three modifications were taken for MD. Selected dock poses were solvated using TIP3P water model in An orthorhombic box. The net electrostatic charge on the solvated model was neutralized and Na+ and Cl− ions were added in concentrations of 0.15 mol/L. Solvated models were energy-minimized using the steepest descent method. Molecular simulation was performed for a period of 200ns for each run at a temperature of 300K and pressure of 1 atm using Nose-Hoover thermostat and Martyna-Tobias-Klein barostat, respectively [35,36]. Simulation was performed with step size of 2 fs in the presence of LINCS harmonic constraints, and the motion was integrated by RESPA integrator. All the visualisations were done on PyMol [37].

2.5. Principal Component Analysis (PCA) and free energy landscaping (FEL)

PCA of protein-ligand complex trajectories were performed using MDTraj programme [38]. Covariance matrix of cartesian coordinates of C-α atoms of protein and heavy atoms of ligands was generated. Eigenvalues and eigenvectors of the covariance matrix were calculated. Ten principal components were extracted using eigenvectors with highest eigenvalues. A 2D Histogram was made based on Principal Component 1 (PC1) and Principal Component 2 (PC2). Free energy landscape was generated from histogram using Boltzmann equation formula: $\Delta E = -k_bT.\ln(n_i/n_{max})$, where n_i is conformation in the ith bin, n_{max} is conformations in maximally occupied bin, ΔE is the energy gap between these conformations, k_b is Boltzmann constant and, T stands for temperature in Kelvin. These FELs were analyzed to get the lowest energy conformational state for each of the ligand-protein complexes. Figure snapshots generated are from these poses.

2.6. Molecular mechanics-generalized born surface area MM-GBSA analysis

MM-GBSA free energy was calculated using average for all frames during the last 10ns of the trajectory using 'Prime MM-GBSA' from Schrodinger [39,40]. Binding energies were calculated from energy differences relating to strain and binding, between ligand, receptor, and ligand-receptor complex using the formula: ΔG Bind = E_complex (minimized) – [(E_ligand (minimized) + E_receptor (minimized)].

2.7. Validation of docking methodology

Crystal structure complex of PI3K-γ with quercetin (**PDB ID 1E8W**) was used for validation of docking methodology. Protein was prepared as receptor and ligand conformation was randomized for docking. RMSD value for best docked pose was compared with crystal structure complex. Kd calculated from the docking score was compared with experimentally available Kd.

2.8. Designing the derivatives of piceatannol and resveratrol

Using piceatannol and resveratrol as scaffold, derivative molecules were generated based on structural analysis of their respective complexes PI3Kγ using the following broad guidelines: (1) modifications were confined to a maximum of three per molecule, (2) nature of functional groups were hydroxyl, amine, carboxyl, and chlorine, (3) positions on the scaffold were based on possibility of the functional groups participating in hydrogen, hydrophobic, ionic, and van der Waals interactions, (4) Lipinski's rule of 5 was adhered to the best extent permissible. These molecules were docked to PI3Kγ, and three most potent derivatives of Piceatannol and Resveratrol were further taken for

Molecular dynamics studies and structural analysis as explained previously. The 2-dimensional structures of native stilbenoids and their derivatives were submitted to SwissADME web tool to delineate the physico-chemical and pharmacokinetic properties [41].

3. Results and discussion

3.1. Sequence analysis

PI3K enzyme comprises of N-terminal adaptor binding domain (ABD), a Ras binding domain (RBD), a C2 linker, a helical domain, and a catalytic kinase domain (Fig. 1A). As the study objective is to develop potent competitive inhibitors at the ATP binding site on the kinase domain, we will mainly focus on the structural analysis of this domain. Primary structures of the kinase domain of the four isoforms γ, α, β, and δ have a minimum of 367 residues and a maximum of 376 residues. These sequences have at least 42 % identity to the γ isoform (Fig. 1B). Catalytic motif that bears the residues Asp-Arg-His-X-X-Asn at positions 946 to 951 on γ-isoform are conserved across all four kinase isoforms. Residues involved in the binding of ATP, wortmannin, myricetin, and quercetin are mostly conserved. Valine is substituted by Isoleucine at position 881, and a neutral Threonine replaces charged residues at position 886 in the γ-isoform. A Lysine doublet is a noticeable variation at 807–808 that is not conserved in the other three isoforms. Role of these variations of the protein on the binding of molecules will be probed in subsequent sections.

3.2. Model building, validation and structural analysis of kinase domain of PI3Kγ

Model of PI3Kγ-isoform is a single polypeptide chain that comprises of a Ras binding domain, C2 linker, Helical domain and catalytic kinase domain (Fig. 1C). PI3Kγ kinase domain consists of two lobes: a smaller N-terminal lobe that comprises 3 α-helices and 5 β-strands, and a larger C-terminal lobe that comprises of 9 α-helices and 3 β-strands. Between these two lobes lies ATP binding pocket with the Ile- Val-Lys-Asp loop adjacent to the substrate binding site (Fig. 1D). Model of kinase domain of PI3K-γ has all the 367 residues in the allowed conformations of Ramachandran plot (Fig. 1E). In addition, ERRAT score of 94.3 % and VERIFY3D score of 69.3 % further validates our model.

3.3. Structures of stilbenoids: piceatannol & resveratrol

Stilbenoids are a hydroxylated derivatives of stilbenes which consists of two benzene rings joined by an ethene group. Due to resonance between the benzene rings and the double bond, stilbenoids tend to have a planar structure. Aromatic ring with the hydroxyl groups is analogous to the adenine, the nitrogen base that has the amine group. Resveratrol is hydroxylated at 1, 3 and 4′ positions whereas piceatannol, a derivative of Resveratrol, is hydroxylated at an additional 3′ position (Fig. 2A and

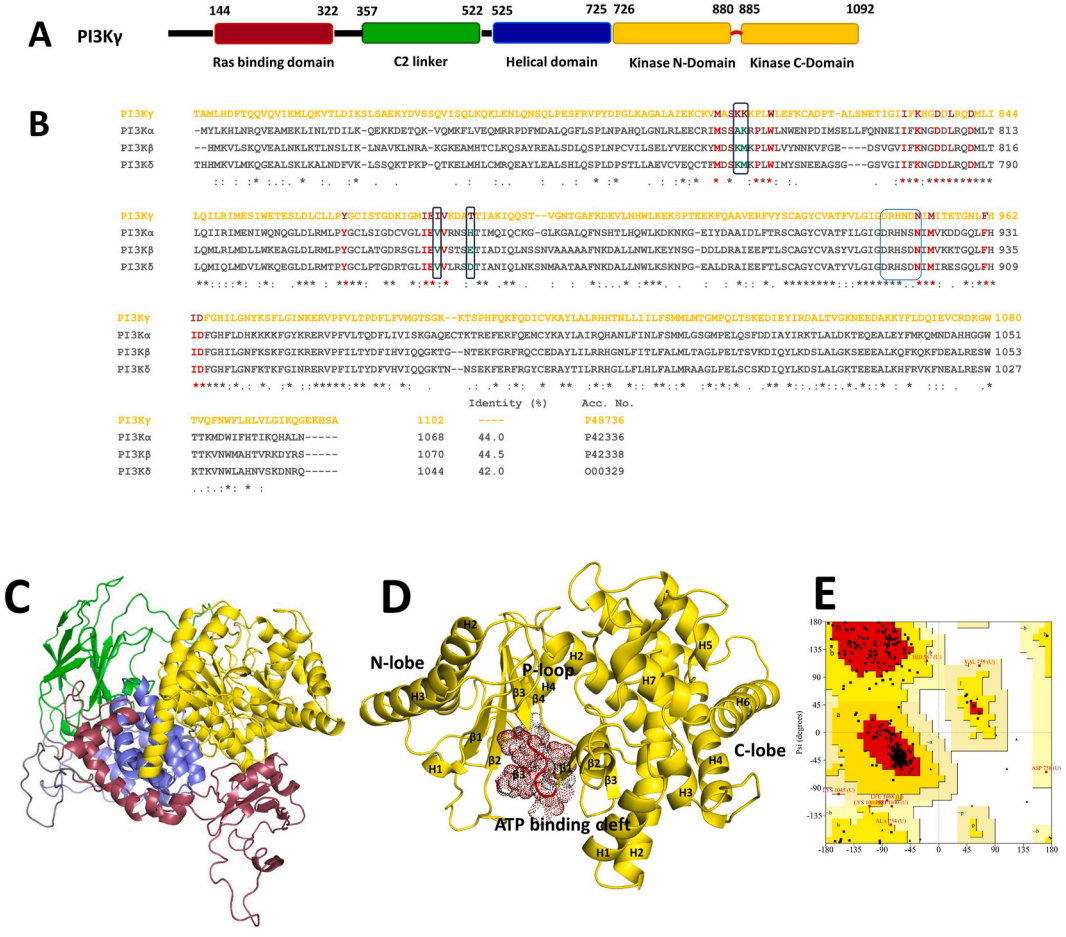

Fig. 1. Sequence analysis (A) Diagrammatic representation of the entire PI3K-γ protein. (B) Multiple sequence alignment of Kinase domain of PI3K-γenzyme isoforms. Residue positions having interactions with Wortmannin, Myricetin, and Quercetin have been highlighted in red in PI3K-γ. The corresponding conserved residues in the other sequences are shown in red and the non-corresponding residues are shown in green. The UniProt accession numbers and percentage identity are shown at the end of the sequences. The symbol '*' indicates identical residues, ':' indicates conserved substitutions and '.' Indicates semi-conserved substitutions. **Structural analysis of PI3K-γ. (C) Ribbon diagram of all the domains of PI3K-γ enzyme, (D) Ribbon diagram showing the Kinase domain with the ATP binding cleft. (E) Ramachandran plots for kinase domain of PI3K**

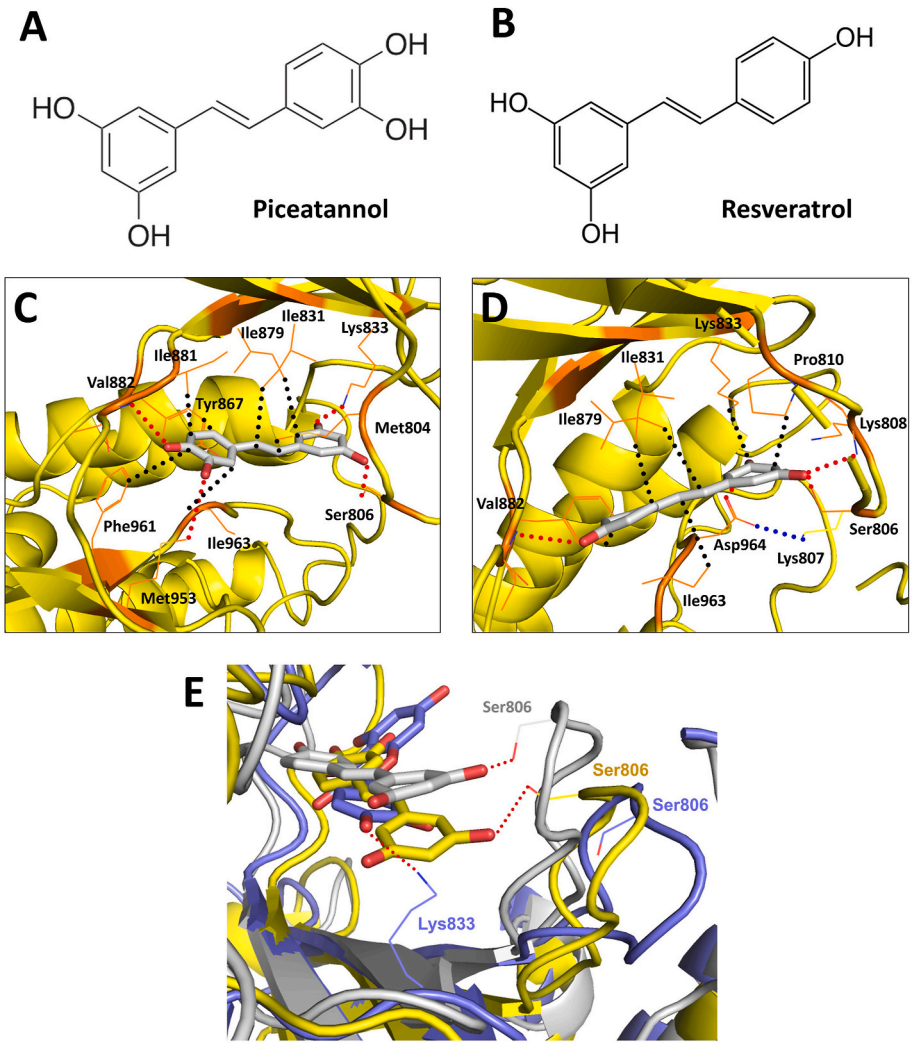

Fig. 2. Structure of stilbenoids. (A) Piceatannol, (B) Resveratrol. Line and stick diagram showing interactions of stilbenoid molecules with PI3K-γ. (C) Residues at the ATP binding site interacting with Piceatannol (D) Residues at the ATP binding site interacting with Resveratrol. Hydrogen bonds are shown as red dotted lines, and ionic bonds are shown as blue dotted lines, and hydrophobic interactions are shown as black dotted lines. **(E) Superimposition of molecules at the ATP binding site of PI3K-γ interaction of Quercetin (purple rendering), Piceatannol (gray rendering) and Resveratrol (yellow rendering) with the P-loops in corresponding colours.**

B). Aromatic rings that have hydroxyl groups at positions 1 and 3 will be called as Ring 1 (R1), and aromatic rings that have hydroxyl groups at positions 4′ and 3' will be called as Ring 2 (R2). Combination of hydroxyl and hydrophobic moieties on these two molecules offer a good possibility of interactions at the ATP binding site of PI3Kγ.

3.4. Structural analysis of complexes of PI3Kγ with piceatannol & resveratrol

Piceatannol and resveratrol bind to PI3Kγ at the ATP binding site. Structural features common to both Piceatannol and resveratrol are: (1) aromatic ring R2 makes edge to face type of pi interactions with the aromatic ring of Tyr867, (2) hydroxyl group on R1 makes a hydrogen bond with Ser806 (PicC3OH…Oγ Ser806), (3) hydroxyl group on 4′ carbon atom forms a hydrogen bond with main chain nitrogen of Val882 (PicC4′O…HN Val882). This is a classical interaction noted in all competitive inhibitor interactions to PI3Kγ at the ATP binding site [9]. It mimics the hydrogen bonded interaction with N1 of adenine in ATP molecule.

Piceatannol, that has two other hydroxyl groups at two ends, of which one is involved in hydrogen bonded interaction with Lys833 (PicR1O…HNζ Lys833). Residues Phe961, Ile881, Ile879, Ile831, Met804, and Ile963 make an array of hydrophobic interactions with carbon atoms along the entire length of Piceatannol (Fig. 2C). These delineated interactions account for the binding of piceatannol to PI3Kγ and explain the functional inhibition of the enzyme by this molecule. Resveratrol that has a hydroxyl group on R1 is involved in hydrogen bonded interaction with Aspartate (ResR1OH…Oδ1 Asp964). Side chain of Asp964 is held in this position by an ionic bond with Lys807 (Fig. 2D). In addition, residues Phe961, Ile963, Ile831, Ile879, Ile881, Trp812, and Pro810 make hydrophobic interactions to stabilize the complex. The quality of these interactions accounts for twice the binding affinity of resveratrol than Piceatannol (Table 1).

Superimposition of these complexes with PI3Kγ-Quercetin complex shows an interesting finding. While the P-loop interaction with Quercetin is absent, the positioning of hydroxyl groups on resveratrol and piceatannol induces a conformational change in the position of P-loop by making hydrogen bonded interactions with Ser806 (Fig. 2E). The rather closed conformation of P-loop results in better compactness and thereby by higher affinities.

As previously discussed, there are certain residues known to interact with ATP and inhibitor molecules such as myrictein, quercetin and wortmannin (Fig. 1B). Many of these conserved residues Met804, Ser806, Pro810, Ile831, Lys833, Asp841, Tyr867, Ile879, Val882,

Table 1
Binding parameters of stilbenoids and their derivatives to kinase domain of PI3Kγ

Molecule	MM-GBSA (kJ/mol)	Kd (nM)	Interacting Residues	Lipinski Rule	Reference
Quercetin (Docked)	–	170	Val882 , Glu880, Asp964, Lys833, Ile963, Ile879, Ile881, Met804 Trp812, Thr887	✓	This study
Quercetin (Experimental)	–	280	Val882 , Glu880, Asp964, Lys833, Ile963, Ile879, Ile881, Met804, Trp812, Thr887	✓	[9]
Alkynylthiazole IP1549	–	0.3	Gly829, Iso881, Trp867, Val882, Lys883, Lys833, Asp884, Asp904	×	[42]
Myricetin	–	170	Val882, Iso881, Tyr867, Asp841, Lys833, Asp964, Iso831, Iso963, Iso879	×	[9]
LY294002	–	210	Val882, Iso881, Tyr867, Lys833, Asp964, Iso831, Iso963, Iso879	✓	[9]
Pyrrolopyridinone	–	3	Val882, Iso881, Tyr867, Asp836, Lys833, Asp964, Iso831, Iso963, Iso879	✓	[43]
Piceatannol	−40.95	200	Val882, Met953, Ser806, Lys833 Ile831, Ile879, Ile881, Ile963, Tyr867, Phe961	✓	This study
PicM07	−52.34	170	Val882, **Glu880**, Asp964, Asp841, **Lys808**, **Lys833**, Leu838, Ile831,Ile879, Ile881, Ile963, Phe961, Met953	×	This study
PicM11	−46.84	50	**Val882**, **Asp841**, **Lys833**, **Lys808**, Tyr867, Ile831, Ile879, Ile881 Ile963	×	This study
PicM12	−49.24	40	Val882, Ile831, Ile963, Tyr867, Ile879, Phe961, Trp812	×	This study
Resveratrol	−59.61	120	Val882, Asp964, Lys808, Ser806, Ile963, Ile879, Ile831, Pro810, Lys833	✓	This study
ResM01	−49.29	20	Val882, **Glu880 (main)**, **Met804**, **Lys833**, **Lys808**, Asp841, Tyr867, Ile831, Ile879, Ile881, Ile963	✓	This study
ResM05	−52.66	30	Val882, **Lys833**, **Lys808**, Asp964 (main), Asp964 (side), Tyr867, Ile879, Ile881, Ile963, Ile831 , Phe961, Met953	✓	This study
ResM06	−56.35	30	**Lys833**, **Lys808**, Asp841, **Glu880 (main)**, **Met804**, Ile879, Ile881 Ile831, Tyr867, Leu838, Asp964	✓	This study

Residues are indicated in Red (Hydrogen bonded interactions), Blue (ionic interactions), Black (hydrophobic), and Bold (interactions arising from modifications)

Met953, Phe961, Ile963, and Asp964 interact with piceatannol and resveratrol. This not only validates our study but places the inhibition of the enzyme by stilbenoids in the right perspective. Among the interacting residues that are not conserved across the other three isoforms, Lys 808 is involved in a hydrogen bonded interaction with resveratrol, and Ile881 is involved in a hydrophobic interaction with piceatannol. Also, Lys807, a non-conserved residue stabilises Asp964 that in turn interacts with resveratrol. These three interactions provide 'sequence-structure' based specificity of these kind of stilbenoid molecules for PI3Kγ enzyme isoform inhibition.

3.5. Structures of stilbenoid derivatives

Based on the structural features of PI3Kγ to Stilbenoids, piceatannol and resveratrol were modified with the aim of achieving a more potent binding and inhibition than that of native molecules. Modifications were governed by certain specific criteria: (1) residue such as Val882 were sought to be engaged in binding interactions, (2) Amine or hydroxyl groups were attached at certain positions to enhance the possibility of hydrogen bonded, Pi-polar interactions, (3) carboxyl group was attached at position 4 for a possible salt bridge with Lys833, (4) Amine group was attached at position 2 to form a salt bridge with Asp841 or Asp964. Derivatives with these combinations were taken up for docking to PI3Kγ at the ATP binding site. Derivatives that showed binding intensities that were comparable to, either the native or previously known inhibitors are shown in Fig. 3.

3.6. Structural analysis of complexes of PI3Kγ with designed derivatives of piceatannol & resveratrol

Derivative molecules are seen to bind at the ATP site just as the native molecules making a lot of interactions with the neighbouring residues (Fig. 3, A-F). Interactions that are most consistent for the six derivative molecules to the residues at the binding site are: (1) hydrogen bonded interaction to the main chain of Val882, (2) ionic interaction between the carboxyl moiety and positive charge on Nζ of Lys833, (3) ionic interaction between the carboxyl moiety and positive charge on Nζ of Lys808, and (4) array of hydrophobic interactions with side chains of Ile831, Ile879, Ile881, Ile963 (Table 1). Modifications on the native molecules are engaged in crucial ionic and hydrogen mediated interactions. Though the chlorine atom on the native molecules is not making any direct interactions with the residues, it looks to be stabilizing the molecules such that strong hydrophobic interactions are established with Met804 (Fig. 3, D&F). The increase in the quantity and quality of interactions of the derivative molecules has helped to improve their potency as compared to the native molecules, Piceatannol and Resveratrol. Though all the six molecules have binding affinities ranging from low micro molar to high nano molar, its only the modified resveratrol molecules that are likely drug candidates as they fulfill the Lipinski criteria. Of the three, ResM05, in addition to the classical interactions with Val882 and Lys833, makes two hydrogen bonded interactions with side chain as well as the main chain of Asp964 (Fig. 3E). The results are therefore convincing for these molecules to be pursued as inhibitor candidates against PI3Kγ.

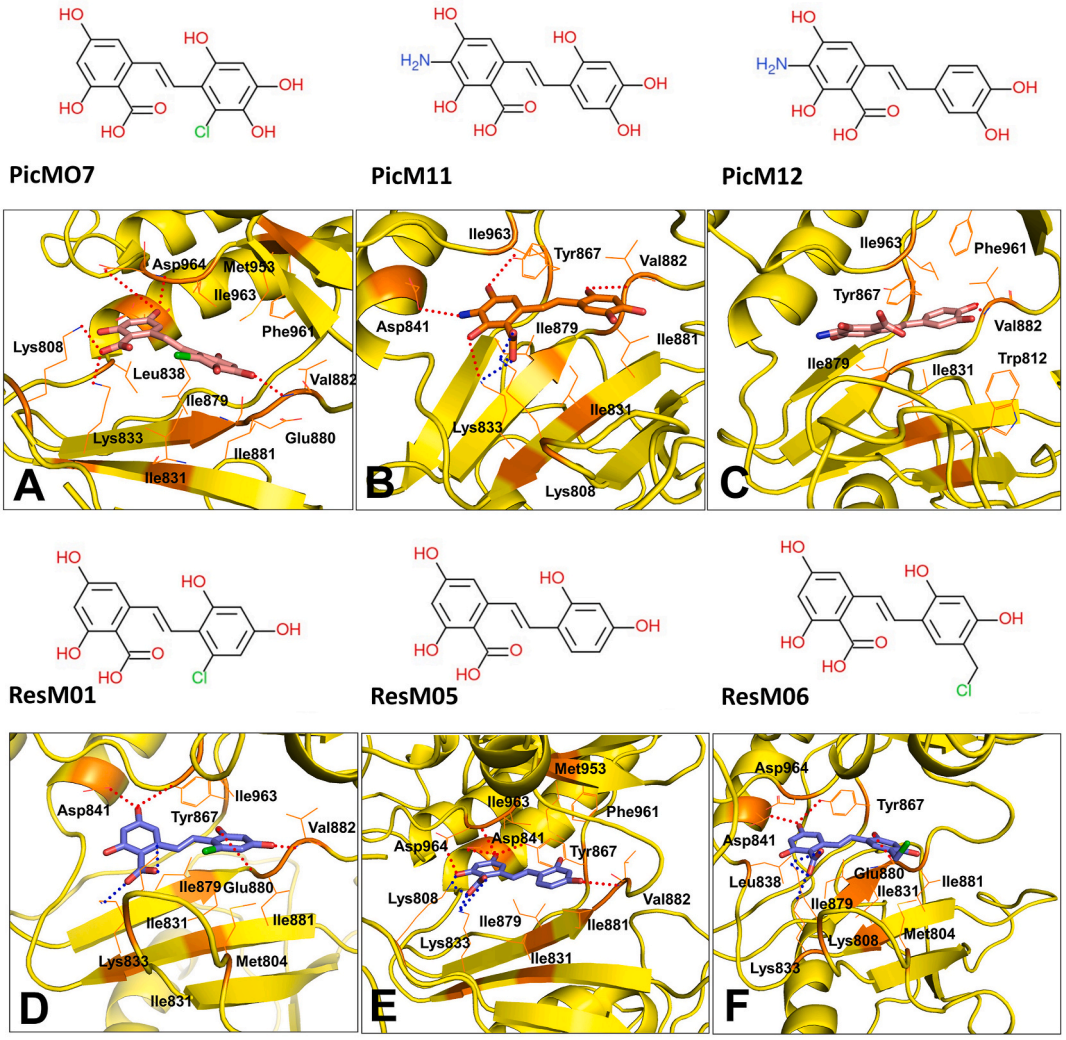

Fig. 3. Structure of designed Stillbenoid derivatives and their interactions with PI3Kγ. (A-C) Piceatannol derivatives, Line and stick diagram showing interactions of Piceatannol derivatives molecules with PI3K-γ. **(D-F)** Resveratrol derivatives; Line and stick diagram showing interactions of Resveratrol derivatives molecules with PI3K-γ. Hydrogen bonds are shown as red dotted lines, and ionic bonds are shown as blue dotted lines, and hydrophobic interactions are shown as black dotted lines. All interactions are in range of 2.5Å - 3.5Å.

3.7. MD trajectory analysis

MD simulation indicates complexes of PI3Kγ with native and derived molecules reached an equilibration state before 50 ns and remained constant thereafter. After equilibration state, RMSD of all complexes converged between 3 Å and 5 Å, which is within thermal vibration range Fig. S1-S3. RMSD of ligands for all the complexes were within 1 Å indicating complexes remained in bound state throughout the trajectory.

Principal Component Analysis (PCA) was used for reduction of parameters of trajectory data sets. PCA based Free Energy Landscapes (FEL) of the complexes were used for analysis of different conformations and their relative stability. While Free Energy Landscapes for complexes with the native molecules showed similar distribution pattern, complexes with derivative molecules showed a more ordered pattern indicating increased stability as shown in Fig. 4. While the derivative molecules of piceatannol showed higher binding affinities compared to the native molecule, the binding energies for resveratrol were more negative than its derivatives. This observation may be attributed to the limitation of the method used for calculating binding energy that does not account for the entropic contribution of Gibbs free energy. The interactions, binding affinities, and drug likeness of the derived stilbenoid molecules are comparable to other previous inhibitors of PI3Kγ such as Quercetin, Alkynylthiazole (IP1549), Myricetin, LY294002, Pyrrolopyridinone (Table 1). Though Pyrrolopyridinone has a dissociation constant of 3 nM, this is a synthetic molecule with diverse biological properties thereby posing a risk of potential side effects and toxicity. Natural stilbenoids and their derivatives proposed in this study are therefore better inhibitor candidates against PI3Kγ.

The physico-chemical and pharmacokinetic properties provide further insights for the molecules to be developed into drug candidates (Table 2). Molecular weight, polar surface area, solubility, lipophilicity, and absorption parameters indicate favourable bio-availability. P-glycoprotein substrate interaction and liver enzyme Cytochrome P450 inhibition give insights into drug metabolism. Lipinski rule, lead likeliness, and synthetic accessibility establish the translational utility of the molecules.

3.8. Validation of docking methodology

Crystal structure of porcine PI3Kγ with Quercetin (**PDB Id: 1E8W**) was used for validating the docking methodology. RMSD of docked complex with crystal structure complex was 0.7Å (Fig. 5). This validates the experimental protocols used in the docking methodology. In

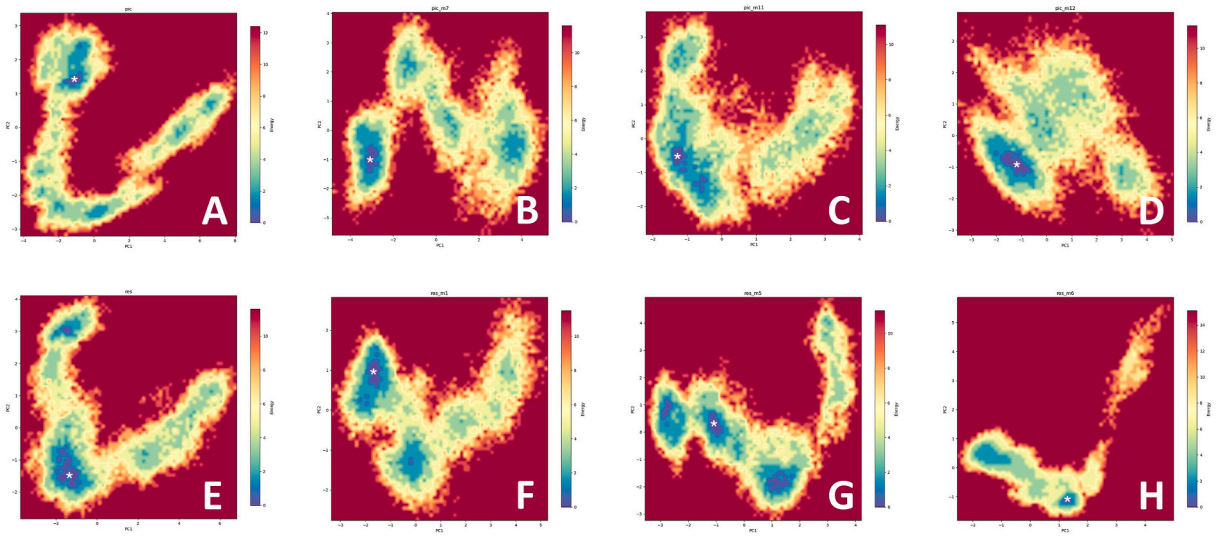

Fig. 4. Comparative free energy landscape (FEL) of PI3Kγ with native stilbenoids molecules and their derivatives. (A) Piceatannol; (B) PicM07, (C) PicM11, (D) PicM12, (E) Resveratrol, (F) ResM01, (G) ResM05, (H) ResM06. Dark blue indicates the lowest energy configuration and red shows the highest energy configuration. White asterix indicates the representative structure used for analysis.

Table 2
Physico-chemical and Pharmacokinetic properties of native stilbenoids and its derivatives

Molecule	Resveratrol	ResM01	ResM05	ResM06	Piceatannol	PicM07	PicM11	PicM12
Formula	C14H12O3	C15H11ClO6	C15H12O6	C16H13ClO6	C14H12O4	C15H11ClO7	C15H13NO7	C15H13NO6
Molecular Weight	228.24	322.7	288.25	336.72	244.24	338.7	319.27	303.27
Aromatic atoms	12	12	12	12	12	12	12	12
Hydrogen-bond acceptors	3	6	6	6	4	7	7	6
Hydrogen-bond donors	3	5	5	5	4	6	7	6
Total polar surface area	60.69	118.22	118.22	118.22	80.92	138.45	164.47	144.24
Consensus Log P (Lipophilicity)	2.48	2.18	1.75	2.35	2.14	1.97	0.63	1.04
Water Solubility	Soluble	Soluble	Soluble	Soluble	Soluble	Soluble	Soluble	Soluble
Gastro-Intestinal absorption	High	High	High	High	High	Low	Low	Low
Blood Brain Barrier permeation	Yes	No	No	No	No	No	No	No
Pgp substrate	No	No	No	No	No	No	No	No
CYP1A2 inhibitor	Yes	No	No	No	Yes	Yes	Yes	Yes
CYP2C19 inhibitor	No	No	No	No	No	No	No	No
CYP2C9 inhibitor	Yes	Yes	Yes	Yes	Yes	Yes	Yes	Yes
CYP2D6 inhibitor	No	No	No	Yes	No	No	No	No
CYP3A4 inhibitor	Yes	No	Yes	Yes	Yes	No	No	Yes
Lipinski #violations	0	0	0	0	0	1	1	1
Bioavailability Score	0.55	0.56	0.56	0.56	0.55	0.56	0.11	0.56
Leadlikeness #violations	1	0	0	0	1	0	0	0
Synthetic Accessibility	Easy	Easy	Easy	Easy	Easy	Easy	Easy	Easy

addition, the binding affinities estimated from this docking study and previous experimental data are comparable (Table 1).

3.9. Limitation of the study

This is a computation based structural bioinformatic study. Crystallization experiments, enzyme inhibition assays and *ex-vivo* studies would help to enhance the credentials of the developed molecules for it to be translated into therapeutics for cancer and inflammation.

4. Conclusion

This study provides a robust structural basis for the binding of natural stilbenoids molecules to PI3Kγ and places the previous enzyme inhibition assays in the right perspective. Biophysical parameters and quality of interactions of stilbenoid derivatives augurs well for development of potent and specific inhibitory molecules against PI3Kγ enzyme.

Disclosure statement

The authors report there are no competing interests to declare.

Data availability statement

The models are available in ModelArchive (modelarchive.org) with the accession codes: PI3Kγ kinase with Piceatannol (ma-43xo4), PI3Kγ kinase with Resveratrol (ma-bcvfm), PI3Kγ kinase with PicM07 (ma-9wnyj), PI3Kγ kinase with PicM11 (ma-goxne), PI3Kγ kinase with PicM12 (ma-aiick), PI3Kγ kinase with ResM01 (ma-y2mtv), PI3Kγ kinase with ResM05 (ma-miknw), and PI3Kγ kinase with ResM06 (ma-lkqv7).

Declaration of competing interest

Authors report no conflict of interest in this work.

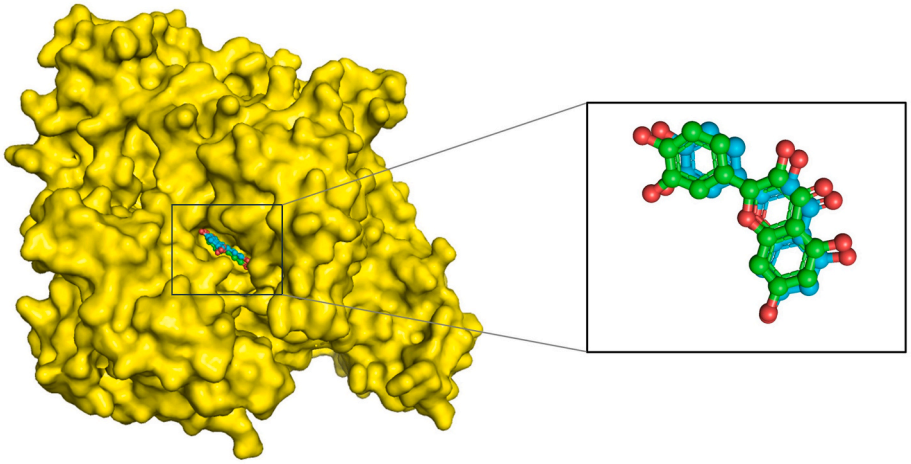

Fig. 5. Validation of docking methodology. Superimposition of crystal structure (PDB ID **1E8W**) (green rendering) and, docked structure (cyan rendering) complexes of PI3K-γ with Quercetin.

Appendix A. Supplementary data

Supplementary data to this article can be found online at https://doi.org/10.1016/j.bbrep.2024.101861.

References

[1] B. Vanhaesebroeck, S.J. Leevers, G. Panayotou, M.D. Waterfield, Phosphoinositide 3-kinases: a conserved family of signal transducers, Trends Biochem. Sci. 22 (1997) 267–272, https://doi.org/10.1016/S0968-0004(97)01061-X.

[2] E. Hirsch, V.L. Katanaev, C. Garlanda, O. Azzolino, L. Pirola, L. Silengo, S. Sozzani, A. Mantovani, F. Altruda, M.P. Wymann, Central role for G protein-coupled phosphoinositide 3-kinase gamma in inflammation, Science 287 (2000) 1049–1053, https://doi.org/10.1126/science.287.5455.1049.

[3] X. Liu, Y. Xu, Q. Zhou, M. Chen, Y. Zhang, H. Liang, J. Zhao, W. Zhong, M. Wang, PI3K in cancer: its structure, activation modes and role in shaping tumor microenvironment, Future Oncol. 14 (2018) 665–674, https://doi.org/10.2217/fon-2017-0588.

[4] B. Vanhaesebroeck, M.A. Whitehead, R. Piñeiro, Molecules in medicine mini-review: isoforms of PI3K in biology and disease, J. Mol. Med. (Berl.) 94 (2016) 5–11, https://doi.org/10.1007/s00109-015-1352-5.

[5] M.J. Zvelebil, L. MacDougall, S. Leevers, S. Volinia, B. Vanhaesebroeck, I. Gout, G. Panayotou, J. Domin, R. Stein, F. Pages, Structural and functional diversity of phosphoinositide 3-kinases, Philos. Trans. R. Soc. Lond. B Biol. Sci. 351 (1996) 217–223, https://doi.org/10.1098/rstb.1996.0019.

[6] B. Bilanges, Y. Posor, B. Vanhaesebroeck, PI3K isoforms in cell signalling and vesicle trafficking, Nat. Rev. Mol. Cell Biol. 20 (2019) 515–534, https://doi.org/10.1038/s41580-019-0129-z.

[7] J. Domin, M.d. Waterfield, Using structure to define the function of phosphoinositide 3-kinase family members, FEBS (Fed. Eur. Biochem. Soc.) Lett. 410 (1997) 91–95, https://doi.org/10.1016/S0014-5793(97)00617-0.

[8] S. Jean, A.A. Kiger, Classes of phosphoinositide 3-kinases at a glance, J. Cell Sci. 127 (2014) 923–928, https://doi.org/10.1242/jcs.093773.

[9] E.H. Walker, M.E. Pacold, O. Perisic, L. Stephens, P.T. Hawkins, M.P. Wymann, R. L. Williams, Structural determinants of phosphoinositide 3-kinase inhibition by wortmannin, LY294002, quercetin, myricetin, and staurosporine, Mol. Cell. 6 (2000) 909–919, https://doi.org/10.1016/s1097-2765(05)00089-4.

[10] R. Mishra, H. Patel, S. Alanazi, M.K. Kilroy, J.T. Garrett, PI3K inhibitors in cancer: clinical implications and adverse effects, Int. J. Mol. Sci. 22 (2021) 3464, https://doi.org/10.3390/ijms22073464.

[11] M. Yu, J. Chen, Z. Xu, B. Yang, Q. He, P. Luo, H. Yan, X. Yang, Development and safety of PI3K inhibitors in cancer, Arch. Toxicol. 97 (2023) 635–650, https://doi.org/10.1007/s00204-023-03440-4.

[12] A.L. Harvey, Natural products in drug discovery, Drug Discov. Today 13 (2008) 894–901, https://doi.org/10.1016/j.drudis.2008.07.004.

[13] M. Feher, J.M. Schmidt, Property distributions: differences between drugs, natural products, and molecules from combinatorial chemistry, J. Chem. Inf. Comput. Sci. 43 (2003) 218–227, https://doi.org/10.1021/ci0200467.

[14] L.M. Hung, J.K. Chen, S.S. Huang, R.S. Lee, M.J. Su, Cardioprotective effect of resveratrol, a natural antioxidant derived from grapes, Cardiovasc. Res. 47 (2000) 549–555, https://doi.org/10.1016/s0008-6363(00)00102-4.

[15] N.R. Ferrigni, J.L. McLaughlin, R.G. Powell, C.R. Smith, Use of potato disc and brine shrimp bioassays to detect activity and isolate piceatannol as the antileukemic principle from the seeds of Euphorbia lagascae, J. Nat. Prod. 47 (1984) 347–352, https://doi.org/10.1021/np50032a019.

[16] F. Wolter, A. Clausnitzer, B. Akoglu, J. Stein, Piceatannol, a natural analog of resveratrol, inhibits progression through the S phase of the cell cycle in colorectal cancer cell lines, J. Nutr. 132 (2002) 298–302, https://doi.org/10.1093/jn/132.2.298.

[17] K.H. Choi, J.-E. Kim, N.R. Song, J.E. Son, M.K. Hwang, S. Byun, J.H. Kim, K.W. Lee, H.J. Lee, Phosphoinositide 3-kinase is a novel target of piceatannol for inhibiting PDGF-BB-induced proliferation and migration in human aortic smooth muscle cells, Cardiovasc. Res. 85 (2010) 836–844, https://doi.org/10.1093/cvr/cvp359.

[18] G. Hariprasad, P. Kaur, A. Srinivasan, T.P. Singh, M. Kumar, Structural analysis of secretory phospholipase A2 from Clonorchis sinensis: therapeutic implications for hepatic fibrosis, J. Mol. Model. 18 (2012) 3139–3145, https://doi.org/10.1007/s00894-011-1333-8.

[19] G. Hariprasad, M. Kumar, P. Kaur, T.P. Singh, R.P. Kumar, Human group III PLA2 as a drug target: structural analysis and inhibitor binding studies, Int. J. Biol. Macromol. 47 (2010) 496–501, https://doi.org/10.1016/j.ijbiomac.2010.07.004.

[20] G. Hariprasad, M. Kumar, K. Rani, P. Kaur, A. Srinivasan, Aminoglycoside induced nephrotoxicity: molecular modeling studies of calreticulin-gentamicin complex, J. Mol. Model. 18 (2012) 2645–2652, https://doi.org/10.1007/s00894-011-1289-8.

[21] G. Hariprasad, A. Srinivasan, R. Singh, Structural and phylogenetic basis for the classification of group III phospholipase A2, J. Mol. Model. 19 (2013) 3779–3791, https://doi.org/10.1007/s00894-013-1913-x.

[22] M.I. Khan, G. Hariprasad, Human secretary phospholipase A2 mutations and their clinical implications, J. Inflamm. Res. 13 (2020) 551–561, https://doi.org/10.2147/JIR.S269557.

[23] F. Sievers, A. Wilm, D. Dineen, T.J. Gibson, K. Karplus, W. Li, R. Lopez, H. McWilliam, M. Remmert, J. Söding, J.D. Thompson, D.G. Higgins, Fast, scalable generation of high-quality protein multiple sequence alignments using Clustal Omega, Mol. Syst. Biol. 7 (2011) 539, https://doi.org/10.1038/msb.2011.75.

[24] A. Šali, T.L. Blundell, Comparative protein modelling by satisfaction of spatial restraints, J. Mol. Biol. 234 (1993) 779–815, https://doi.org/10.1006/jmbi.1993.1626.

[25] J.U. Bowie, R. Lüthy, D. Eisenberg, A method to identify protein sequences that fold into a known three-dimensional structure, Science 253 (1991) 164–170, https://doi.org/10.1126/science.1853201.

[26] C. Colovos, T.O. Yeates, Verification of protein structures: patterns of nonbonded atomic interactions, Protein Sci. 2 (1993) 1511–1519, https://doi.org/10.1002/pro.5560020916.

[27] R.A. Laskowski, M.W. MacArthur, D.S. Moss, J.M. Thornton, PROCHECK: a program to check the stereochemical quality of protein structures, J. Appl. Crystallogr. 26 (1993) 283–291, https://doi.org/10.1107/S0021889892009944.

[28] R. Lüthy, J.U. Bowie, D. Eisenberg, Assessment of protein models with three-dimensional profiles, Nature 356 (1992) 83–85, https://doi.org/10.1038/356083a0.

[29] T.J. Dolinsky, J.E. Nielsen, J.A. McCammon, N.A. Baker, PDB2PQR: an automated pipeline for the setup of Poisson-Boltzmann electrostatics calculations, Nucleic Acids Res. 32 (2004) W665–W667, https://doi.org/10.1093/nar/gkh381.

[30] A.D. MacKerell, D. Bashford, M. Bellott, R.L. Dunbrack, J.D. Evanseck, M.J. Field, S. Fischer, J. Gao, H. Guo, S. Ha, D. Joseph-McCarthy, L. Kuchnir, K. Kuczera, F. T. Lau, C. Mattos, S. Michnick, T. Ngo, D.T. Nguyen, B. Prodhom, W.E. Reiher, B. Roux, M. Schlenkrich, J.C. Smith, R. Stote, J. Straub, M. Watanabe, J. Wiórkiewicz-Kuczera, D. Yin, M. Karplus, All-atom empirical potential for molecular modeling and dynamics studies of proteins, J. Phys. Chem. B 102 (1998) 3586–3616, https://doi.org/10.1021/jp973084f.

[31] M.H.M. Olsson, C.R. Søndergaard, M. Rostkowski, J.H. Jensen, PROPKA3: consistent treatment of internal and surface residues in empirical pKa predictions, J. Chem. Theor. Comput. 7 (2011) 525–537, https://doi.org/10.1021/ct100578z.

[32] J. Eberhardt, D. Santos-Martins, A.F. Tillack, S. Forli, AutoDock Vina 1.2.0: new docking methods, expanded force field, and Python bindings, J. Chem. Inf. Model. 61 (2021) 3891–3898, https://doi.org/10.1021/acs.jcim.1c00203.

[33] K.J. Bowers, D.E. Chow, H. Xu, R.O. Dror, M.P. Eastwood, B.A. Gregersen, J. L. Klepeis, I. Kolossvary, M.A. Moraes, F.D. Sacerdoti, J.K. Salmon, Y. Shan, D. E. Shaw, Scalable algorithms for molecular dynamics simulations on commodity clusters, in: SC '06: Proceedings of the 2006 ACM/IEEE Conference on Supercomputing, 2006, p. 43, https://doi.org/10.1109/SC.2006.54, 43.

[34] E. Harder, W. Damm, J. Maple, C. Wu, M. Reboul, J.Y. Xiang, L. Wang, D. Lupyan, M.K. Dahlgren, J.L. Knight, J.W. Kaus, D.S. Cerutti, G. Krilov, W.L. Jorgensen, R. Abel, R.A. Friesner, OPLS3: a force field providing broad coverage of drug-like small molecules and proteins, J. Chem. Theor. Comput. 12 (2016) 281–296, https://doi.org/10.1021/acs.jctc.5b00864.

[35] A.C. Branka, Nose-Hoover chain method for nonequilibrium molecular dynamics simulation, Phys. Rev. E 61 (2000) 4769–4773, https://doi.org/10.1103/physreve.61.4769.

[36] G.J. Martyna, D.J. Tobias, M.L. Klein, Constant pressure molecular dynamics algorithms, J. Chem. Phys. 101 (1994) 4177–4189, https://doi.org/10.1063/1.467468.

[37] L.L.C. Schrödinger, The PyMOL Molecular Graphics System, 2020, Version 2.4.

[38] R.T. McGibbon, K.A. Beauchamp, M.P. Harrigan, C. Klein, J.M. Swails, C. X. Hernández, C.R. Schwantes, L.-P. Wang, T.J. Lane, V.S. Pande, MDTraj: a modern open library for the analysis of molecular dynamics trajectories, Biophys. J. 109 (2015) 1528–1532, https://doi.org/10.1016/j.bpj.2015.08.015.

[39] F. Adasme-Carreño, C. Muñoz-Gutierrez, J. Caballero, J.H. Alzate-Morales, Performance of the MM/GBSA scoring using a binding site hydrogen bond network-based frame selection: the protein kinase case, Phys. Chem. Chem. Phys. 16 (2014) 14047–14058, https://doi.org/10.1039/C4CP01378F.

[40] F. Chen, H. Liu, H. Sun, P. Pan, Y. Li, D. Li, T. Hou, Assessing the performance of the MM/PBSA and MM/GBSA methods. 6. Capability to predict protein–protein binding free energies and re-rank binding poses generated by protein–protein docking, Phys. Chem. Chem. Phys. 18 (2016) 22129–22139, https://doi.org/10.1039/C6CP03670H.

[41] A. Daina, O. Michielin, V. Zoete, SwissADME: a free web tool to evaluate pharmacokinetics, drug-likeness and medicinal chemistry friendliness of small molecules, Sci. Rep. 7 (2017) 42717, https://doi.org/10.1038/srep42717.

[42] U.K. Bandarage, A.M. Aronov, J. Cao, J.H. Come, K.M. Cottrell, R.J. Davies, S. Giroux, M. Jacobs, S. Mahajan, D. Messersmith, C.S. Moody, R. Swett, J. Xu, Discovery of a novel series of potent and selective alkynylthiazole-derived PI3Kγ inhibitors, ACS Med. Chem. Lett. 12 (2021) 129–135, https://doi.org/10.1021/acsmedchemlett.0c00573.

[43] J.H. Come, P.N. Collier, J.A. Henderson, A.C. Pierce, R.J. Davies, A. Le Tiran, H. O'Dowd, U.K. Bandarage, J. Cao, D. Deininger, R. Grey, E.B. Krueger, D. B. Lowe, J. Liang, Y. Liao, D. Messersmith, S. Nanthakumar, E. Sizensky, J. Wang, J. Xu, E.Y. Chin, V. Damagnez, J.D. Doran, W. Dworakowski, J.P. Griffith, M. D. Jacobs, S. Khare-Pandit, S. Mahajan, C.S. Moody, A.M. Aronov, Design and synthesis of a novel series of orally bioavailable, CNS-penetrant, isoform selective phosphoinositide 3-kinase γ (PI3Kγ) inhibitors with potential for the treatment of multiple sclerosis (MS), J. Med. Chem. 61 (2018) 5245–5256, https://doi.org/10.1021/acs.jmedchem.8b00085.